Solid Suspension and Liquid Phase Mixing in Solid−Liquid Stirred Tanks

Madhavi V. Sardeshpande,[†,‡] Aparna R. Sagi,[§] Vinay A. Juvekar,[‡] and Vivek V. Ranade*,[†]

Industrial Flow Modeling Group, National Chemical Laboratory, Pune-411 008, India, Department of Chemical Engineering, Indian Institute of Technology Bombay, Powai, Mumbai-400076, India, Tridiagonal Solutions Pvt. Ltd., 100 NCL Innovation Park, Pune 411008, India, and National Institute of Technology, Surathkal, Karnataka-575 025, India

Stirred tanks are widely used in chemical process industries for catalytic reactions, dissolution of solids, crystallization, and so on. In designing and optimizing such processes, suspension quality of slurry is an important parameter. Suspension quality depends upon complex interactions of impeller generated flow, turbulence, and solid loading. Most of the earlier work on solid suspension focuses on identifying critical impeller speed for just suspension of solids (N_{js}). In this study, apart from N_{js}, aspects like cloud height and liquid phase mixing in solid−liquid suspensions were also studied. A new way of characterizing solid−liquid suspensions and liquid phase mixing using nonintrusive wall pressure fluctuation measurements has been developed. Systematic experimental data on N_{js}, cloud height, power consumption, mixing time, and circulation time over a range of solid volume fraction and impeller speeds have been presented here. The results and discussion presented here will have useful implications for designing solid−liquid stirred tanks.

1. Introduction

Stirred tanks are widely used in chemical process industries for catalytic reactions, dissolution of solids, crystallization, and so on. The quality of suspension in slurry reactors is a very crucial parameter in designing and optimizing in such processes. Conventionally, solid suspension in stirred reactors is characterized by the "just suspension impeller" speed required for a just off-bottom suspension (N_{js}). This N_{js} is the speed at which all particles are lifted up from bottom of the vessel and not spending more than 1 or 2 s on the bottom of the vessel.[1] Though the concept of N_{js} was introduced fifty years ago (after the work of Zwietering in 1958[1]), it is still used as a primary design parameter even today. Design of a solid−liquid stirred vessel relies on an empirical correlations obtained from experimental data. Zwietering[1] proposed the correlation for determination of N_{js} by flow visualization from the bottom of the vessel. A number of experimental studies was reported in the literature after Zwietering[1] to explain the effect of solid loading and particle size on N_{js}.[2−6] Despite 50 years of research, there are still significant discrepancies in defining and predicting suspension quality. An attempt is made here to characterize suspension quality using cloud height, liquid phase mixing time, and liquid phase circulation time in solid−liquid stirred vessels using conventional as well as advanced methods.

The quality of solid suspension can be broadly divided into three regimes, i.e., on-bottom (partial), off-bottom (complete), and homogeneous (uniform) suspension regimes.[7] As agitation begins in the solid−liquid system, one can visually observe the solid−liquid interface at a certain distinct level. The distinct level at which most of the solids gets lifted within the fluid where the solid−liquid interface appears is called the "cloud height". Measurement of cloud height within the stirred vessel provides a qualitative indication of suspension quality. Kraume,[8] Hicks et al.,[9,10] Bujalski et al.,[11] and Takenaka et al.[12] provided extensive data on cloud height measurements. The model developed by Bittorff and Kresta[13] showed monotonic increase of cloud height with increase in impeller speed. Meanwhile, Takenaka et al.[12] observed nonmonotonic behavior such as the cloud height decreased with an increase in impeller speed and, with further increase in impeller speed, cloud height was found to increase. As discrepancies are observed in reported studies, it is necessary to shed some light on cloud height measurements and enhance the physical understanding behind solid suspension in a stirred vessel.

Unambiguous methods for estimating power requirements for solid−liquid stirred tanks are not available. The general approach usually adopted in the available literature makes use of the available correlation for a single phase power number, N_p (based on liquid density), and for a two phase power number, N_p (based on liquid density), or N_{ps} (based on slurry density) to predict power requirements in slurry systems. Experimental data[14−19] of power dissipation of solid−liquid systems depended on solids concentration, impeller geometries, and particle size. Disagreements were observed in reported N_p, and its variation with key operating and design parameters. For example, Rewatkar et al.[14] and Michelletti et al.[19] reported increase in N_p with increasing impeller speed. Pinelli et al.[15] observed decrease in N_p with increase in impeller speed. Bubicco et al.[16] reported an increase of N_{ps} with increase in solid concentration. Drewer at al.[17] reported that N_{ps} was a function not only of solid concentration but also of particle size. Mak[18] studied effect of particle size and concluded that N_p increased with increasing particle size. In contrast, Barresi and Baldi[20] observed that, for same volume fraction, the N_p was lower for large particles as compared to small particles. In short, reported studies showed scattered information about effect of key parameters on power consumption in a solid−liquid slurry system. Hence, an attempt was made here to study key parameters such as solid concentration, particle size, impeller speed/type, and power consumption.

In the case of solid−liquid systems, Joshi[21] has calculated average circulation velocity on the basis of mixing time and maximum length of circulation loop. The circulation velocity obtained in this manner agrees well with the experimentally measured values, and hence, an exactly reverse procedure can be followed to calculate the mixing time in practice. McManamey[22]

* To whom correspondence should be addressed. Tel./Fax: +91-20-64015548. E-mail: vv.ranade@tridiagonal.co.in.
† National Chemical Laboratory.
‡ Indian Institute of Technology Bombay.
§ Tridiagonal Solutions Pvt. Ltd and National Institute of Technology.

has explained successfully the use of average liquid circulation velocity and maximum loop length on mixing time to explain the effect of various parameters. Joshi et al.[23] have mentioned that mixing time is inversely proportional to average circulation velocity where the longest circulation loop exists. They also added that mixing time is equal to 5 times the circulation time which indicates that five circulations are required for the achievement of 99% of liquid phase mixing. In addition to this, there are some recent reports mentioning the relationship between delayed mixing and cloud height.[8,11,18,24–26,32] Therefore, in the present study, effect of cloud height on mixing time was studied using two conductivity probes, i.e. one was near the surface and one was at impeller clearance. An attempt was made in the work to explore the link between mixing time and circulation time for various solid loading.

The dynamics of fluidized beds and bubble column reactors have been studied using wall pressure fluctuations by several investigators.[27–31] They have used the embedding techniques based on the Takens[32] study and applied them to time-delay coordinate expansions to provide a way to reconstruct and characterize the underlying dynamics and ultimately to define a criteria for regime identification. Drahos et al.[33] proposed a simple parametric method for a purpose of online flow pattern identification using the autoregressive model. The focus was ultimately on correlating properties of the time series by means of a set of scaling exponents. Briens and Briens[34] have developed a method to study cycle characteristics of a measured time series. They have used V statistics and P statistics (calculated from Hurst analysis) to detect the flow regime transitions in multiphase systems such as risers and gas–solid and gas–liquid–solid fluidized beds. On the basis of that, Khopkar et al.[35] had used a wall pressure fluctuation technique for flow regime identification in a gas–liquid stirred tank reactor. None of the studies has reported the detailed characterization of solid–liquid flows in a stirred reactor to provide information of the underlying fluid dynamics and to define criteria for regime identification. In this study, an attempt was made to estimate circulation/cycle time for mentioned operating and design parameters.

Exploring a possibility of using a nonintrusive technique, i.e. wall pressure fluctuations, to characterize solid suspension (regimes) was the objective of the present work. Similar methodology[35] was adopted to identify flow regimes of solid–liquid suspensions in a stirred reactor. The method was also extended to estimate key time scale i.e. cycle/circulation time of solid suspension and relate this to mixing time.

Characterization of solid–liquid systems was done using a pilot plant scale experimental setup and different measurement techniques that are discussed in section 2. The results are discussed in section 3, and the key findings of the present work are highlighted in the conclusion.

2. Experimental Section

Experiments were carried out in a fully baffled, flat bottom cylindrical reactor (diameter, $T = 0.7$ m, $H/T = 1$). Pictorial view and a schematic diagram of the experimental setup are shown in Figure 1. Four baffles of width $T/10$ were mounted diametrically opposite and perpendicular to the reactor wall. A shaft of an impeller ($d_s = 0.032$ m) was concentric with an axis of the reactor. A down pumping 6-bladed pitched blade turbine (PBTD-6) and 4-bladed Hydrofoil (HF-4) impellers (of diameter, $D_i = 0.2$ m) were used in this work. The impeller off-bottom clearance was ($C = T/3$) measured from the middle of the impeller blade height. Glass bead particles ($\rho_s = 2500$
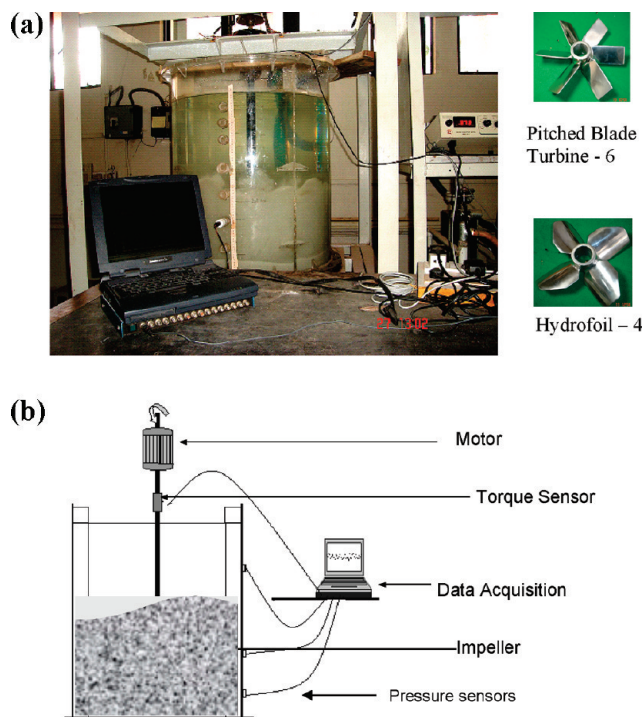

(a)

Pitched Blade Turbine - 6

Hydrofoil – 4

(b)

Motor

Torque Sensor

Data Acquisition

Impeller

Pressure sensors

Figure 1. Experimental setup with axial flow impellers. (a) Pictorial view. (b) Schematic view.

kg/m³) of diameter 50 and 250 μm were used. Experiments were carried out for four different solid loadings viz 1, 3, 5, and 7% v/v. The working fluid was tap water ($\rho_l = 1000$ kg/m³) in all experiments. Measurements were carried out for ten different impeller speeds ranging from 150 to 602 rpm. Selected operating conditions for PBTD-6 and HF-4 covered all suspension regimes occurring in the solid–liquid stirred tank reactor. Measurement techniques such as visual observations, torque fluctuations, wall pressure fluctuations, and liquid phase mixing time are discussed briefly in the following subsection.

2.1. Flow Visualization. Flow visualization was done by two different methods: one is Zwietering's[1] method (i.e., placing a mirror below the bottom of the tank), and the second is Kraume's[8] method (i.e., from the side wall of the vessel) for investigation of just suspension impeller speed (N_{js}). A sample of photographs is shown in Figure 2. Both visualization methods provided useful qualitative indications of solid distribution/ suspension. Impeller speed was varied from 150 to 602 rpm that was decided by calculating N_{js} using Zwietering's[1] correlation. It was also observed that cloud height was not uniform across the diameter of tank and varies appreciably with time due to unsteady flow behavior. Therefore, after attainment of quasisteady state, the range of cloud height variation was noted down. The arithmetic mean of upper and lower limits of this range was considered as the mean height of cloud and is reported in this work.

2.2. Torque Fluctuations. A precalibrated torque sensor (with a range from 0 to 50 N m and sensitivity of 1.59 mV/ (N m)) was used (Mechanica systems, India) to measure instantaneous strain values developed on shaft. Measured strain values were then transmitted to the data acquisition system in the form of a voltage signal via a telemetry system which was further acquired on a laptop, using a 16-bit A/D PCMCIA converter card and data acquisition software, "dAtagate" (of nCode, UK). Instantaneous voltage values were acquired with a sampling frequency of 400 Hz for a period of 400 s. Data was processed with the help of a calibration chart (voltage to
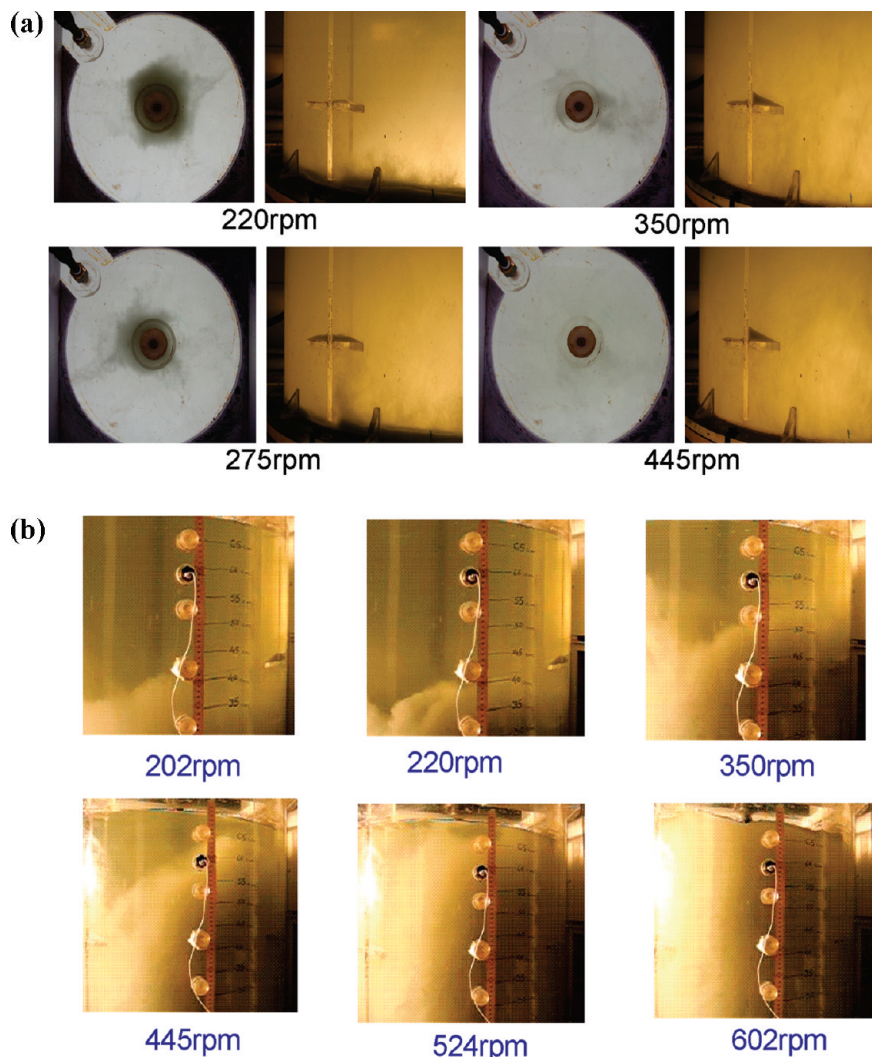
(a)

220rpm   350rpm

275rpm   445rpm

(b)

202rpm   220rpm   350rpm

445rpm   524rpm   602rpm

Figure 2. Visual observations (a) using Zwietering's method and (b) using Kraume's method.

torque) to obtain time the averaged value of the total torque. In the present work, power number (N_P) calculated on the basis of liquid phase density as well as using slurry density.

$$P = 2\Pi N \frac{1}{n} \sum_{i=1}^{n} (T'_i) \tag{1}$$

$$N_P = \frac{P}{\rho_l N^3 D^5} \quad \text{and} \quad N_P = \frac{P}{\rho_{mix} N^3 D^5} \tag{2}$$

2.3. Liquid Phase Mixing Time. A conductivity meter was used to measure liquid phase mixing time in the solid−liquid stirred reactor. The conductivity cell (of Electronics India Ltd., India, Model 601E) was mounted 2 cm inside the tank wall to measure the time history of passive tracer concentration, of 1 molar NaCl salt solution of volume equal to 0.3% of the total reactor volume. For denser slurry systems, mixing time depended upon the distinct level of the solid−liquid interface (i.e., cloud height). Therefore, two conductivity probe locations were selected for this study: one was at impeller clearance level ($z = 23.33$ cm from bottom), and the second one was near the surface ($z = 65$ cm from bottom). For each experiment, a pulse of salt solution was added into reactor at the liquid surface and conductivity time history was recorded for each probe. Time histories of tracer concentration values were acquired with a

sampling frequency of 100 Hz and for the period of 250 s. The measured time history (series) of tracer concentration was first amplified and then transmitted to the data acquisition system. Considering the limitations of the available conductivity probe, different solid loadings, external electronic noise, and recorded time history for tracer concentration, homogeneity criteria was used as ±15% of the final concentration (C_∞). The time required to attain the desired homogeneity from an instance at which tracer was added is called the "mixing time (θ_{mix})". The reproducibility of mixing time was verified by repeating all experiments three times.

2.4. Wall Pressure Fluctuations. A pressure transducer (with a range of ±34.46 kPa, resolution of 0.000 482 kPa, and sensitivity of 72.54 mV/kPa) was used (PCB Piezoelectronics Inc., USA, Model 106B50) to measure wall pressure fluctuations. This transducer was flush mounted on the reactor wall at a height of impeller off-bottom clearance. This transducer was powered by ICP battery unit (PCB Piezoelectronics Inc., USA, Model 480E06), which acted as an amplifier. Wall pressure fluctuations were acquired with a sampling frequency of 400 Hz and for a period of 400 s. The acquired time series of wall pressure fluctuations were analyzed by using in-house code "Analysis of nonlinear Time Series, AnTS".[36] The acquired time series were first low pass filtered[37] and were then normalized with an average absolute deviation. It was ensured that low pass

filtering did not remove any useful information in the signal (the differences in root-mean square (rms) values of filtered and unfiltered series were less than 1−2%). Typical raw and filtered time series was shown in Figure 3a. The power spectral density function (PSD) was calculated using a standard fast Fourier transform (FFT) algorithm.[37] The power spectrum indicates relative strengths of different frequencies at three axial locations. However, in many cases it was not possible to identify the single dominant frequency from the power spectrum for the solid−liquid system for higher solid loading (see Figure 3b). It was found that power spectrum can identify the cycle time only of periodic or nearly periodic time series.

Therefore, Hurst[38] developed a method to quantify the persistence of time series. It divides the time series in intervals of time length τ. A rescaled range is calculated for each interval. The average of rescaled ranges (R/S) can then be obtained for all intervals of length (τ). Changing the value of interval length τ and plotting $\ln(R/S)$ as a function of $\ln(\tau)$ gives a curve whose slope is the Hurst exponent H. According to Peters,[39] if a time series exhibits cyclic behavior, the Hurst exponent H changes at certain values of τ and the plot of $\ln(R/S)$ vs $\ln(\tau)$ is not a straight line. The change in slope corresponds to the cycle (circulation) time. He developed a more generalized statistical tool such as P-statistics for analysis of nonperiodic time series.

The P statistics are defined as

$$P_\tau = \frac{(R/S)_\tau}{\tau^\gamma} \tag{3}$$

Where, γ is calculated as

$$\gamma = \text{maximum } P \text{ statistics} - \frac{\text{maximum of } P \text{ statistics at the minimum and maximum } \tau}{\text{maximum of } P \text{ statistics at the minimum and maximum } \tau} \tag{4}$$

The optimized value of γ calculated was 0.7. Therefore, P statistics was used for determination of cycle time (circulation time). It is defined as the time required to complete one cycle over a reference distance, that time is cycle time. A detailed procedure is explained well by Briens and Briens[34] to identify cycle time. The average fluid circulation velocity was calculated using this circulation time for justification of the could height in solid−liquid systems as follows.

$$\text{circulation time} = \frac{\text{longest loop length}}{\text{fluid circulation velocity}} \tag{5}$$

$$\text{fluid circulation velocity} = \frac{\text{longest loop length}}{\text{circulation time}} \tag{6}$$

Longest loop length was considered as developed fluid flow up to a certain height (i.e., nothing but cloud height for a solid−liquid system) for a corresponding impeller speed as well as solid loading. This loop length as well as the time required to complete one cycle changes depending upon solid loading and impeller speed. This provided information about the fluid circulation velocity.
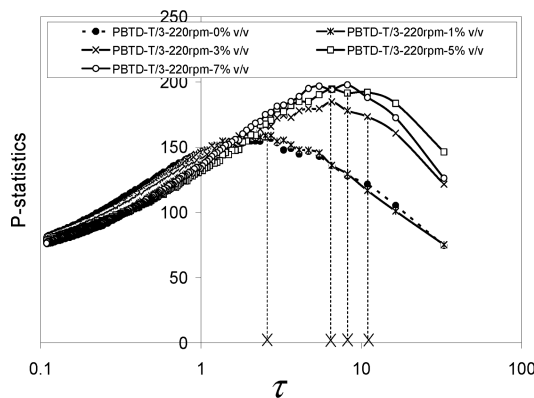
The same methodology was adopted here, and a sample plot for 220 and 602 rpm is as shown in Figure 3c and d and ultimately N_{js} and N_{us} for suspension regimes. It was observed that higher characteristic cycle times for increasing solid loading
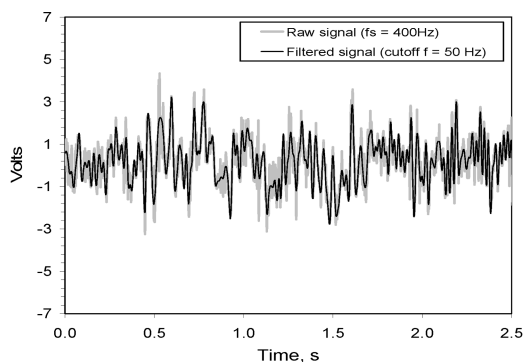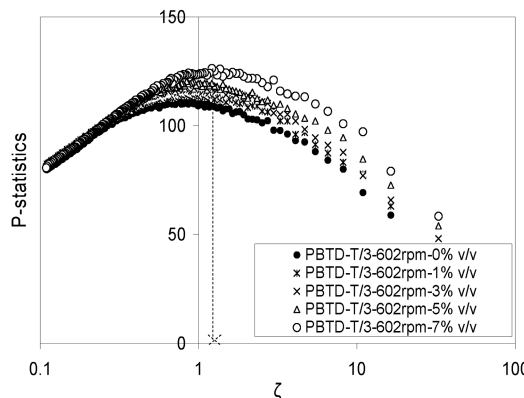

(a) Raw and filtered data of time series
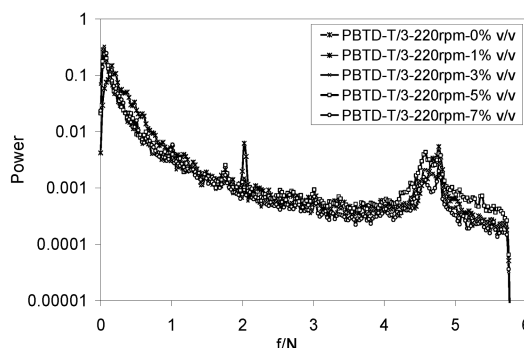
(b) Power spectral analysis at various solid loadings

(c) P-statistics at 220rpm

(d) P-statistics at 602rpm

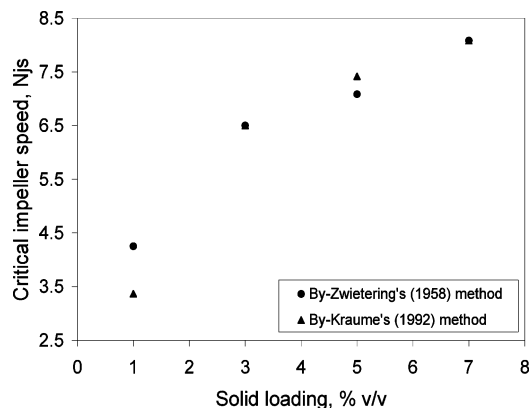**Figure 3.** Analysis of time series using wall pressure fluctuation technique.

Figure 4. Estimation of just suspension impeller speed using visual methods.

indicated the presence of a solid bed on the bottom of the vessel and required more time to follow the liquid flow path. Whereas at 602 rpm and for all solid loadings, characteristics cycle time was the same, i.e. 1.1 s. The P statistics curve at 602 rpm showed an almost equal contribution of impeller generated flow and solid loading to overall fluid dynamics. It was observed that the same cycle time means being directed toward a fully developed flow pattern, negligible effects of solid loading, and also an approximately uniform suspension regime.

3. Results and Discussion

As discussed earlier, suspension quality is interdependent upon different operating and design parameters. Results and key findings from the present work are discussed in the following.

3.1. Effect of Impeller Speed and Solid Loading. Impeller speed and solid loading are interlinked parameters and playing vital role in suspension of solids in stirred tank.

Visual observation experiments were carried out following Zwietering's[1] as well as Kraume's[8] method. Application of Zwietering's[1] method (observing at the vessel bottom) becomes difficult at higher solid loadings even with increased impeller speed because differentiation of the transition from the partly suspended to just suspended condition was gradual. Thus, identification of N_{js} was difficult and impractical at higher solid loadings. Kraume's[8] method of observing the cloud of particles from the front view was easier. It also provided information regarding solid deposition/suspension in the corners of the tank wall, total height of suspended slurry (i.e., cloud height), and also N_{js} for different solid loadings. Quantitatively, N_{js} obtained from both methods are found to agree with each other within ±8% as shown in Figure 4.

Discrepancies were observed in cloud height measurements; those of Hick et al.[9,10] showed monotonic increase in cloud height with increasing impeller speed. Britoff and Kresta[13] proposed a model for the prediction of cloud height that also predicted monotonic increase in cloud height with increasing impeller speed.

$$CH = \frac{N}{N_{js}}\left[0.84 - 1.05\frac{C}{T} + 0.7\frac{(D/T)^2}{(1 - (D/T)^2)}\right] \quad (7)$$

It is true that the model is applicable for cloud heights (CHs) from 0.6 to 0.9T and for N greater than N_{js}. In this work, it was just an attempt to compare existing experimental results with the model and to verify the usefulness of the model for different stages of solid suspension at various solid loadings. Our results are compared with the results predicted by the Britoff and
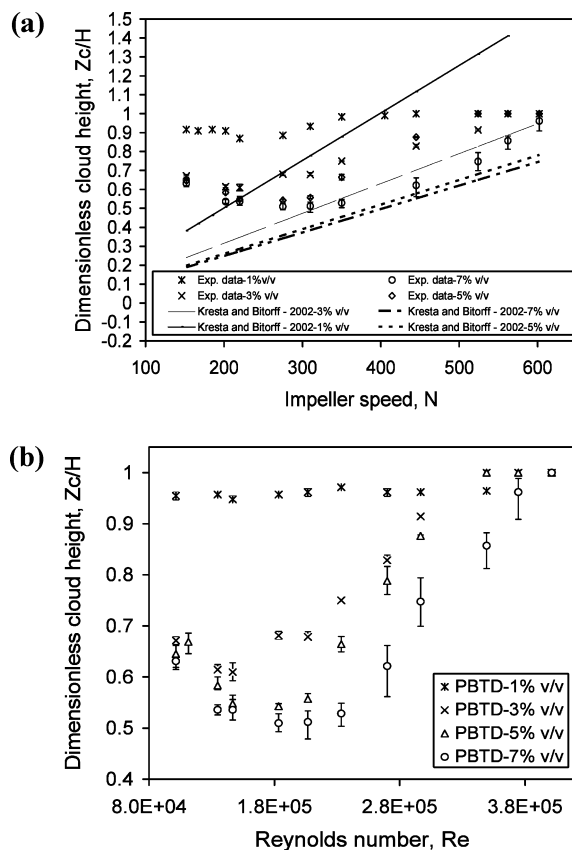

Figure 5. (a) Comparative study of cloud height measurements with the proposed model. (b) Cloud heights measurements at various solid loadings using PBTD-6.

Kresta[13] model (see Figure 5a). Takenaka et al.[12] however reported nonmonotonic behavior of cloud height with increasing impeller speed. They observed four different stages of cloud height with increased impeller speed. In the present work, we also observed nonmonotonic behavior of cloud height with increase in impeller speed.

In the present work, cloud height measurements were done for 1–7% v/v solid loading. It was observed that the influence of impeller speed on cloud height was not significant at a solid volume fraction of 1% v/v. At dilute suspension (i.e., 1% v/v), for all impeller speeds, dimensionless cloud height (Z_c/H) approximately remained same, i.e. between 0.9 and 1. The influence of impeller speed on cloud height was clearly visible from the data collected at solid volume fraction equal or above 3% v/v (Figure 5b). It was also observed that cloud height decreased as solid loading increased above 3% v/v. This was because with increased solid loading, the height of solid bed on bottom also increased (i.e., effective off-bottom clearance decreased) and it affected the suspension of particles and liquid circulation velocity. For example, at 3% v/v, cloud height was found to decrease with impeller speed in the range 150–220 rpm (i.e. $Re \approx 1$–1.47×10^5). At 150 rpm, visually it was observed that most of the solids were settled at the vessel bottom. A small fraction of solid particles was suspended up to significant height in the vessel. With increase in impeller speed to 220 rpm speed, flow stream from impeller impinges on the settled solid bed leading to suspension of more solid particles. This resulted into two significant recirculation zones: (1) from the vessel bottom to the impeller and (2) impeller to top surface. In first recirculation zone, visually observed slurry density was more than that in other recirculation zones. As a result of this, the liquid circulation velocity decreased and already suspended
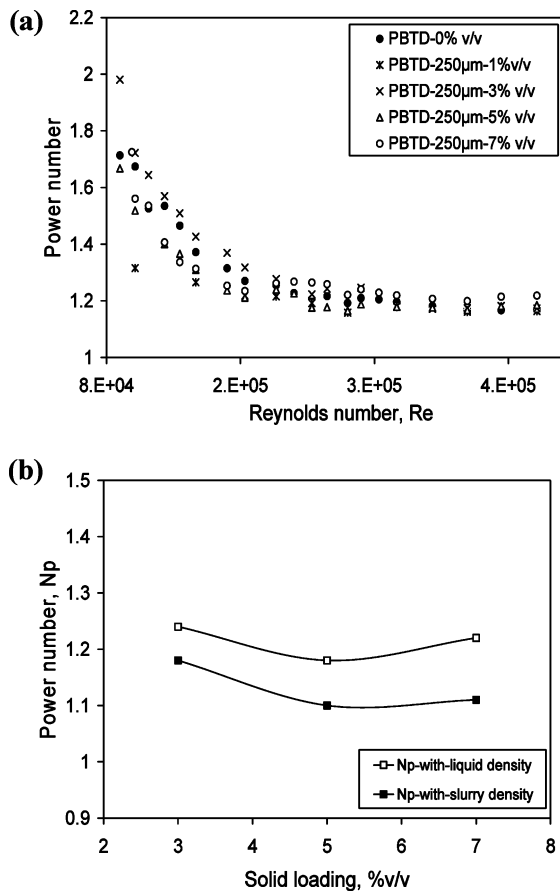
(a)

(b)

Figure 6. (a) Effect of impeller speed on power number. (b) Effect of solid loading on power number.

particles tended toward settling. Therefore, cloud height decreased as impeller speed increased. When impeller speed increased beyond 220 rpm (i.e. $Re \approx 1.47-2.97 \times 10^5$), cloud height increased with increase in impeller speed.

This physical phenomenon was confirmed by circulation time measurements using the wall pressure fluctuations technique (discussed in the next section). At 150 rpm (i.e. $Re \approx 1.01 \times 10^5$), the average fluid circulation velocity was $0.043U_{tip}$. However, at 220 rpm (i.e. $Re \approx 1.47 \times 10^5$), the average fluid circulation velocity was found to be $0.021U_{tip}$ (that is even in absolute terms velocity is lower than that at 150 rpm). Fluid circulation velocity was calculated as discussed in section 2.4. Thus, with further increase in impeller speed beyond 220 rpm, the bed region below the impeller which reduces the strength of impeller flow stream vanishes and further increase in impeller speed leads to better flow (increased circulation velocity i.e. $0.021-0.085U_{tip}$) resulting into better suspension and higher cloud heights. At 445 rpm (i.e. $Re \approx 2.97 \times 10^5$), solids are more or less uniformly suspended and therefore further increase in impeller speed does not affect the cloud height and cloud height remains constant with further increase in impeller speed.

Variation of power number with respect to solid loadings was also measured over a range of impeller speeds. The usual way of plotting is in dimensionless form, i.e. N_p vs Re for all solid loadings. It was observed that with increasing impeller speed, i.e. from $Re \sim 9 \times 10^4$ to 2.7×10^5, power number decreased for single phase. Thereafter, from $Re \sim 2.7-4 \times 10^5$, power number remained constant. In the case of a two phase, i.e. solid−liquid, system, N_p was calculated based on liquid density as well as slurry density. An attempt was made here, to compare qualitative as well as quantitative trends in N_p vs Re curve for
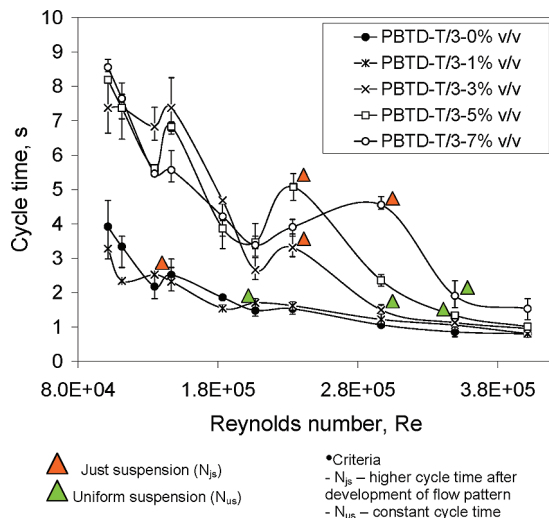

Figure 7. Effect of impeller speed on cycle time at various solid loadings.
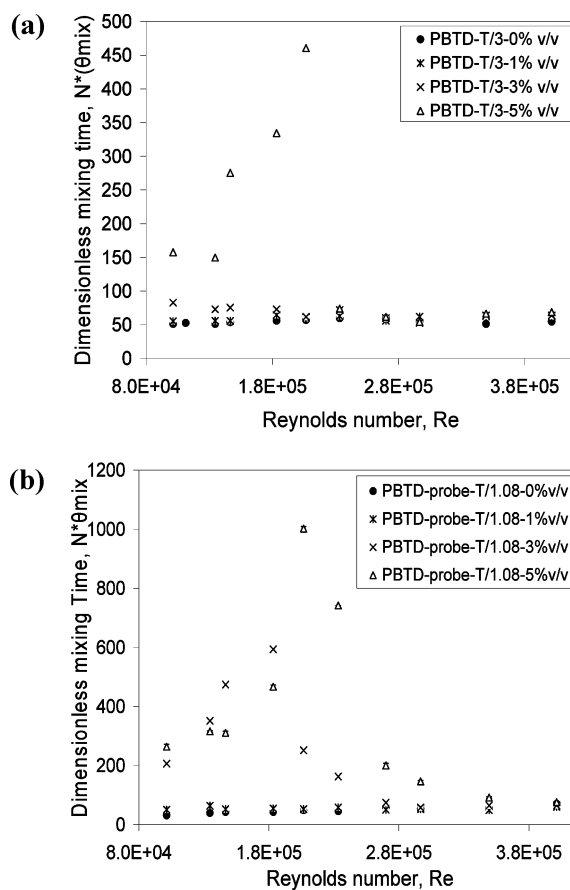
(a)

(b)

Figure 8. (a) Dimensionless mixing time at probe location $T/3$, i.e. impeller clearance. (b) Dimensionless mixing time at probe location $T/1.08$, i.e. near the surface.

all solid loadings (see Figure 6a). It was found out that N_p started decreasing with increasing Re and remained approximately constant once there was uniform suspension of particles. The qualitative trends observed in variation of N_p with solid loading were similar (Figure 6b).

Wall pressure fluctuation measurement was used in the present work for determination of suspension regimes in denser solid−liquid systems. A statistical tool, i.e. P statistics, of pressure fluctuations was used to identify cycle time for range impeller speed and solid loading (as discussed in section 2.4).
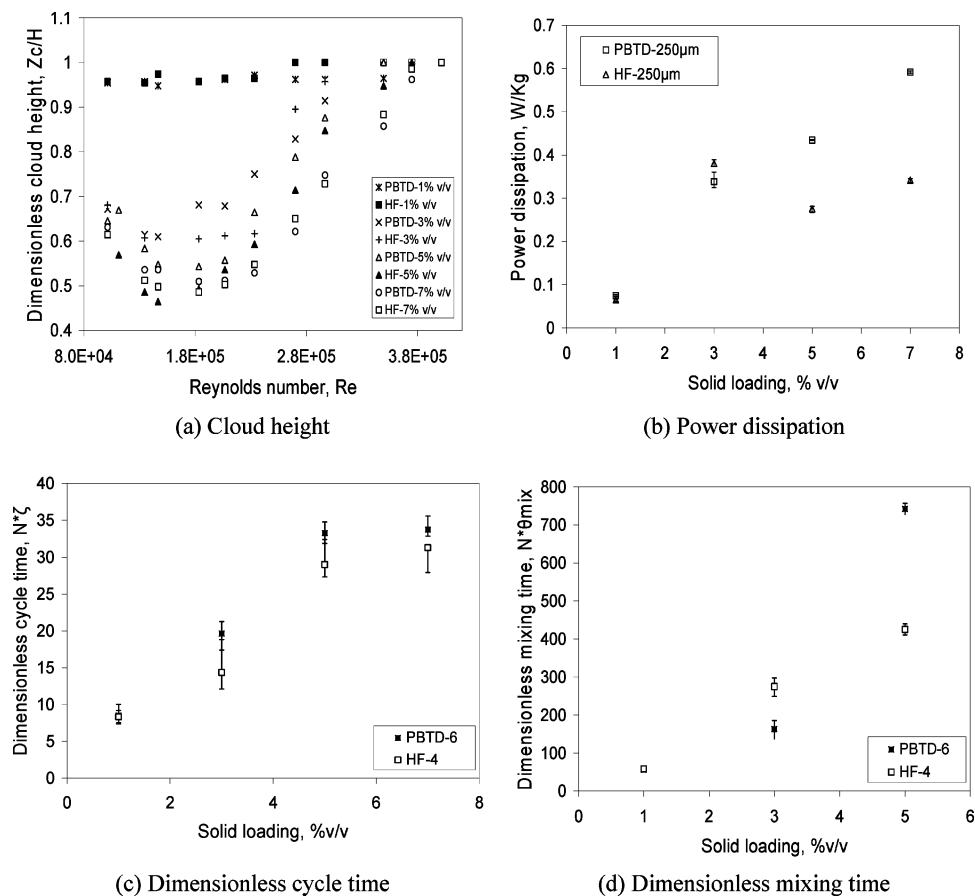
(a) Cloud height

(b) Power dissipation

(c) Dimensionless cycle time

(d) Dimensionless mixing time

Figure 9. Effect of impeller type at various solid loadings (results in b−d are at N_{js}).

Characteristic cycle time was estimated from the time scale associated with the maximum P statistics value which means that a change in slope in the P statistics vs τ curve indicated completion of a cycle inside the vessel. It indicated that characteristic cycle time for 0 and 1% v/v was same, i.e. 2.5 s showing fully developed flow pattern inside the tank. Whereas, for 3, 5, and 7% v/v solid loading at 220 rpm, characteristic cycle times were higher, i.e., 5.62, 6.82, and 7.37 s, respectively. Similarly, for a range of impeller speeds, characteristic cycle time for all solid loading was estimated and is shown in Figure 7. It can be seen that characteristic cycle time decreases with increase in impeller speed at the beginning (this is the phase when solids are not suspended). With further increase in impeller speed, there was a sudden increase in cycle time indicating suspension of particles (with corresponding impact on reduction in pumping number). Further increase in impeller speed results in better solids suspension (increased cloud height) and therefore shows reduction in cycle time. When impeller speed increases beyond a certain point (where uniform solid suspension occurs), the product of cycle time and impeller speed remains constant. Observed influence of impeller speed on characteristics circulation time at different solid loadings and estimations of N_{js} and N_{us} based on this data are shown in Figure 7.

Characteristic circulation time could be one of the possible ways to get liquid phase mixing time for a solid−liquid system (as per the available literature). For verification and exploration of the link between circulation time and mixing time scales, experiments were carried out to estimate the liquid phase mixing time in a stirred tank reactor. Liquid phase mixing time for 0 and 1% v/v solid loading was decreased with increasing impeller speed whereas for 3 and 5% v/v solid loading, the liquid phase mixing time depended upon the height of the solid−liquid
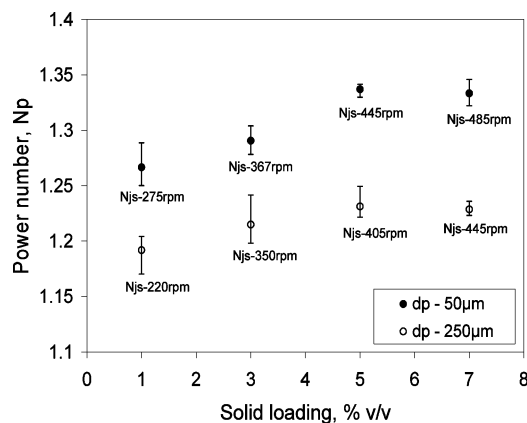

Figure 10. Effect of particle size on power number at various solid loadings.

interface (i.e., cloud height). In the present work, similar to Harrop et al.[25] and Kasat et al.,[40] we also observed delayed mixing (higher mixing time) with increasing solid loading (see Figure 8a and b). These experiments were carried out by using two different axial probe locations to acquire quantitative information about θ_{mix}. With these two conductivity probes, two different mixing times were observed, i.e. 9.16 and 129.5 s for 3% v/v at 275 rpm and 77.35 and 193.8 s for 5% v/v at 310 rpm. With these experiments, it was confirmed that there was a development of a weak secondary flow loop in the clear fluid at the upper part of the vessel which affects the overall liquid phase mixing time of the system. A qualitative trend was found since both of the probes were same but quantitatively mixing time was higher in the case of the upper probe location depending upon the cloud height as well as solid loading
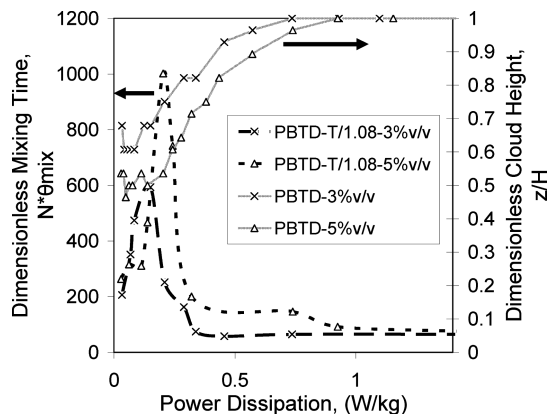
Figure 11. Comparative study of cloud height and liquid phase mixing time and corresponding power dissipation for 3 and 5% v/v solid loadings.

Figure 13. Just suspension impeller speed using various techniques and reported correlations.
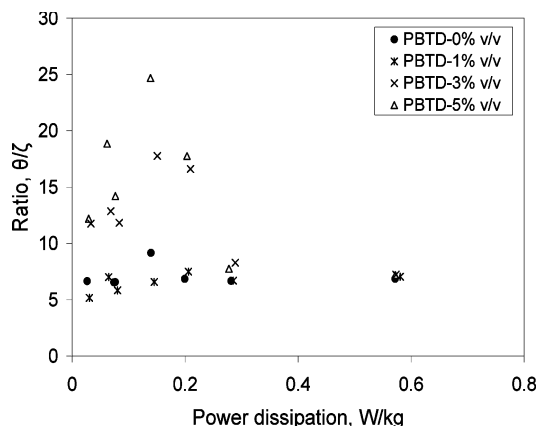

Figure 12. Comparative study of ratio of mixing and cycle time.

(see Figure 8a and b). Because of the existence of such different mixing scales in cloud height and upper clear liquid layer, for all the solid loadings considered here, as impeller speed increases, θ_{mix} was also found to increase. The mixing time was found to attain a maximum value at some impeller speed and with further increase in impeller speed θ_{mix} dropped gradually and remained inversely proportional to the impeller speed beyond a certain impeller speed. The impeller speed where the θ_{mix} vs impeller speed curve changes its trend indicated about "just-suspension" conditions, i.e. N_{js} for respective solid loadings.

3.2. Effect of Impeller Type and Particle Size. The effect of impeller type was studied using a down pumping 6-bladed pitched blade turbine (PBTD-6) and 4-bladed Hydrofoil (HF-4) impellers. Both impellers were used to characterize the solid−liquid system at mentioned operating conditions. A comparative study of qualitative as well as quantitative trends was done for cloud height, power consumption, and circulation time as well as liquid phase mixing time measurements. It was observed that quantitative information estimated from cloud height measurements for both types of impellers were in the range of ±8% (see Figure 9a). The measured power consumption, circulation time, and mixing time for these two impellers as a function of solids loading at just suspension conditions are shown in Figure 9b−d, respectively. It can be seen from Figure 9b that PBTD-6 and HF-4 required approximately the same power for 1 and 3% v/v solid loadings. For 5% and 7% v/v solid loadings, PBTD-6 required 36−42% more power than HF-4. Characteristic circulation time and mixing time for the two impellers are shown in Figure 9c and d, respectively. It was
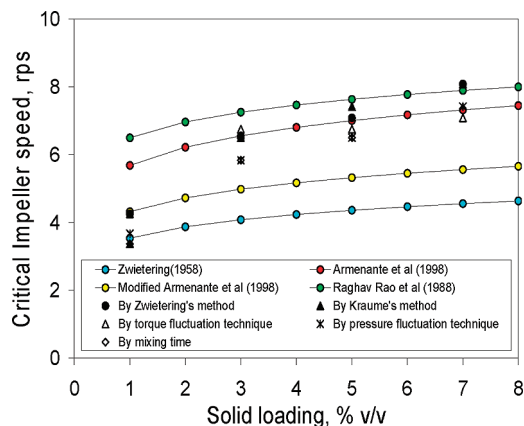
found out that circulation time values measured for both the impellers were more or less the same (i.e., within error bars). The measured mixing time at N_{js} showed marked difference at solids loading of 5%. It may be noted that the circulation time values were estimated by a pressure sensor located at the impeller level whereas mixing time values were estimated by a conductivity probe located near the top surface. This may explain different observed behavior with respect to circulation time and mixing time.

The effect of particle size was studied using two sizes of particles, i.e. 50 and 250 μm. Cloud height measurements were possible in the case of the 250 μm size particles. However, for 50 μm size particles, cloud height measurement was not possible because of the milky and opaque nature of the slurry.

The qualitative trend for power number (N_p) as a function of Reynolds number (Re) for the 50 and 250 μm size particles was similar. Quantitatively, N_p for the 50 μm size particle was more than that of the 250 μm size particle as shown in Figure 10. This result is in agreement with the study of Barasi and Baldi.[20]

The effects of different operating parameters were studied for the characterization of a solid−liquid system in a stirred tank reactor (suspension quality). It was thought desirable that a systematic comparative study of cloud height, power consumption, circulation time, and link between circulation time and mixing time would provide useful information on suspension quality in the solid−liquid slurry reactors. This is discussed in the following.

3.3. Comparative Study. The methods presented in this work can be used to understand the influence of solid loading and impeller speed on state of suspension, just suspension impeller speed, and characteristic time scales. Torque fluctuation and wall pressure fluctuation based methods rely on statistical analysis and are independent of fluid properties, opaqueness, and scale of the vessel. The techniques presented here could be used with commercially available industrial torque and pressure sensors. The analysis and detection of just suspension impeller speed was fairly straightforward and unambiguous. These techniques provided a comprehensive understanding of cloud height, mixing time, cycle time, and power consumption. A sample of these results is discussed in the following.

Suspension quality was characterized using cloud height and liquid phase mixing time. These results are shown in Figure 11 as a function of power dissipation. It was observed that the 90% cloud height criteria developed by Kraume[8] corresponds with a constant value of $N\theta_{mix}$ for 3% v/v solid loading. However, this was not the case for 5% v/v solid loading. It was proposed

that measurement of cycle time via wall pressure fluctuations may allow for quicker estimation of mixing time. Hence, the ratio of the measured liquid phase mixing time and circulation time was examined (see Figure 12). This ratio was found to be in the range of 5−7 for liquid (single phase) as well as for 1% v/v solid loading (i.e., two-phase). For solid loading over and above 3% v/v, this ratio (θ/τ) was found to change with the impeller speed and cloud height. At higher solid loadings and at certain impeller speeds, this ratio was found as high as ∼20. This was mainly due to the delayed mixing observed in the clear liquid region above the cloud height. The cycle time was obtained from a pressure sensor located at the impeller level, and it was therefore not able to capture larger time scales in the low velocity clear liquid region above the cloud height. This led to significantly higher ratio of mixing time to cycle time. As impeller speed increases further (at higher power dissipation), cloud height increases and eventually this ratio again falls in the range of 5−7.

Comparison of the just suspension impeller speed estimated from different techniques mentioned here and estimations of some of the reported correlations is shown in Figure 13. It was found that measurements with different techniques agreed within 11% of each other. At lower solid loading, our results are closer to those estimated using Zweitering's[1] correlation. At higher solid loading (>3%v/v), our results are closer to those estimated using Raghav Rao et al.[2] and Armanante et al.[6] correlations. The wall pressure fluctuation technique used in this work can potentially be used for carrying out measurements of just suspension impeller speed, suspension regimes, and circulation time in large, opaque industrial systems.

4. Conclusions

Experiments were carried out to characterize solid−liquid suspension using measurements of cloud height, power consumption, liquid phase mixing, and circulation time for solid loadings up to 7% v/v using PBTD-6 and HF-4. The key conclusions based on this work are listed in the following:

(a) At higher solid loading (on and above 3% v/v), cloud height measurements indicated different stages of suspension. Cloud height was found to decrease with increase in impeller speed under certain conditions. Interaction of incompletely suspended solids, bed of unsuspended solids at the bottom and impeller pumping action causes such nonmonotonic variation of cloud height with the impeller speed.

(b) The power number for 50 μm size particles was found to be 6−8% higher than that for 250 μm size particles.

(c) The power required for just suspending the particles by a down flow pitched blade impeller (PBTD-6) was found to be about 40% higher than that by a hydrofoil impeller (HF-4).

(d) Mixing time (θ_{mix}) was found to depend on cloud height and on solid loading (when solid loading is above 3% v/v).

(e) The wall pressure fluctuations technique was found to be useful to quantify different suspension regimes and to estimate characteristic circulation time.

(f) Characteristics circulation time estimated from wall pressure fluctuations can provide useful indications on mixing time in suspension regimes where there is no significant clear liquid region above the solids cloud.

Notations

P = power, W
N = impeller speed, rps
N_{js} = just suspension impeller speed, rps

N_{us} = impeller speed at uniform suspension, rps
$N_p = N_p$ (considering liquid density, ρ_l)
$N_{ps} = N_p$ (considering slurry density, ρ_{mix})
D = impeller diameter, m
$P_T = P$ statistics
(R/S) = rescaled range
T_i = instantaneous torque, N m

Greek Letters

γ = exponent of P statistics
ρ = density of water, kg/m^3
τ = cycle (circulation) time, s
θ_{mix} = mixing time, s

Literature Cited

(1) Zwietering, Th. N. Suspending of Solid Particles in Liquid by Agitators. *Chem. Eng. Sci.* **1958**, *8*, 244.

(2) Raghava Rao, K. S. M. S.; Rewatkar, V. B.; Joshi, J. B. Critical impeller speed for solid suspension in mechanically agitated contactors. *AIChE J.* **1988**, *34*, 1332.

(3) Sharma, R. N.; Shaikh, A. A. Solid suspension in stirred tanks with pitched blade turbines. *Chem. Eng. Sci.* **2003**, *58*, 2123.

(4) Armenante, P. M.; Nagamine, E. U. Effect of low off-bottom impeller clearance on the minimum agitation speed for complete suspension in stirred tanks. *Chem. Eng. Sci.* **1998**, *53*, 1757–1775.

(5) Nienow, A. W. Suspension of solid particles in turbine-agitated baffled vessels. *Chem. Eng. Sci.* **1968**, *23*, 1453.

(6) Armenante, P. M.; Nagamine, E. U.; Susanto, J. Determination of correlations to predict the minimum agitation speed for complete solid suspension in agitated vessels. *Can. J. Chem. Eng.* **1998**, *76*, 413–419.

(7) Paul, E. L., Atiemo-Obeng, V. A.; Kresta, S. M. *Handbook of industrial mixing - science and practice*; John Wiley and Sons: New Jersey, 2004.

(8) Kraume, M. Mixing times in stirred suspension. *Chem. Eng. Technol.* **1992**, *15*, 313.

(9) Hicks, M. T.; Mayers, K. J.; Bakker, A. Cloud height in solid suspension agitation. *Chem. Eng. Commun.* **1997**, *160*, 137.

(10) Hicks, M. T.; et al. Cloud height, fillet volume and the effect of multiple impellers in solid suspension. Presented at *Mixing XIV*, Santa Barbara, CA, June 20−25, 1993.

(11) Bujalski, W.; Takenaka, K.; Paolini, S.; Jahoda, M.; Paglianti, A.; Takahashi, K.; Nienow, A. W.; Etchells, A. W. Suspension and liquid homogenization in high solids concentration stirred chemical reactors. *Trans. Inst. Chem. Eng.* **1999**, *77*, 241.

(12) Takenaka, K.; Takashi, K.; Bujalski, W.; Nienow, A. W.; Paolini, S.; Pagaltini, A.; Etchells, A. Mixing time for different diameters of impeller at a high solid concentration in an agitated vessel. *J. Chem. Eng. Jpn.* **2005**, *38* (5), 309.

(13) Bittorf, K. J.; Kresta, S. M. Prediction of cloud height for solid suspension in stirred tanks. *CHISA Conference Proceedings*, Prague, Aug. 25, 2002.

(14) Rewatkar, V. B.; Joshi, J. B. Critical Impeller Speed for Solid Suspension in Mechanically Agitated Three-Phase Reactors. 2. Mathematical Model. *Ind. Eng. Chem. Res.* **1991**, *30*, 1784.

(15) Pinelli, D.; Nocentini, M.; Magelli, F. Solids distribution in stirred slurry reactors: influence of some mixer configurations and limits to the applicability of a simple model for predictions. *Chem. Eng. Commun.* **2001**, *188*, 91–107.

(16) Bubicco, R.; Di Cave, S.; Mazzarotta, B. Influence of solid concentration and type of impeller on the agitation of large PVC particles in water. *Recents Prog. Genie Procedes* **1997**, *11* (52), 81.

(17) Drewer, G. R.; Ahmed, N.; Jameson, G. J. Suspension of high concentration solids in mechanically stirred vessels. *AIChE Symp. Ser.* **1994**, *136*, 41.

(18) Mak, A. T. C.; Ruszkowski, S. W. Scaling up solids distribution in stirred vessels. *IV Fluid Mixing, AIChE Symp. Ser.* **1991**, *121*, 379.

(19) Michelletti, M.; Nikiforaki, L.; Lee, K. C.; Yianneskis, M. Particle concentration and mixing characteristics of moderate-to-dense solid-liquid suspensions. *Ind. Eng. Chem. Res.* **2003**, *42*, 6236.

(20) Barresi, A.; Baldi Power consumption in slurry systems. *10th European Conference on Mixing*, Delft, the Netherlands, July 2−5, 2000; p 133.

(21) Joshi, J. B. Axial mixing in multiphase contactors - A unified correlation. *Trans. Inst. Chem. Eng.* **1980**, *58*, 155.

(22) McManamey, W. J. Circulation model for batch mixing in agitated baffled vessel. *Trans. Inst. Chem. Eng.* **1980**, *58*, 271.

(23) Joshi, J. B.; Pandit, A. B.; Sharma, M. M. Mechanically agitated gas-liquid reactors. *Chem. Eng. Sci.* **1982**, *37* (6), 813–844.

(24) Nienow, A. W.; Bujalski, K.; Takenaka, A.; Paglianti, S.; Paolini, M.; Jahoda; Etchells, A. W. Suspension and Liquid Homogenization in High Solids Concentration Chemical Reactors. *Proceedings of the International Conference on Mixing and Crystallization*, Tioman Island, Malaysia, April, 1998.

(25) Harrop, K. L.; Spanfelner, W. H.; Jahoda, M.; Otomo, N.; Etchells, A. W.; Bujalski, W.; Hicks, M. T.; Mayers, K. J.; Bakker, A. Cloud height, fillet volume, and effect of multiple impellers in solid suspension. Presented at *Mixing XIV*, Santa Barbara, CA, June 20−25, 1993.

(26) Takenaka, K.; Paglianti, A., Bujalski, W.; Nienow, A. W. Suspension at High Solid Concentrations in agitated vessels. *Proceedings of the Institute of Chemical Engineers Research Event*, University of Newcastle upon Tyne, U.K., 1998; Catalyst Electronic Publishing, Ltd.: Witney, U.K., 1998; CD Rom.

(27) Franca, F.; Acikgoz, M.; Lahey, R. T.; Clausse, A. The use of fractal techniques for flow regime identification. *Int. J. Multiphase Flow* **1991**, *17*, 545.

(28) Daw, C. S.; Halow, J. S. Modelling deterministic chaos in gas-fluidized beds. *AIChE Symp. Ser.* **1992**, *88* (289), 61.

(29) Van der Stappen, M. L. M.; Schouten, J. C.; van den Bleek, C. M. Deterministic chaos analysis of the dynamical behavior of slugging and bubbling fluidized beds. *Fluidized Bed Combust.* **1993**, *1*, 129.

(30) Schouten, J. C.; Van den Bleek, C. M. Monitoring the quality of fluidization using the short term predictability of pressure fluctuations. *AIChE J.* **1998**, *44*, 48–60.

(31) Letzel, H. M.; Schouten, J. C.; Krishna, R.; van den Bleek, C. M. Characterization of regimes and regime transitions in bubble columns by chaotic analysis of pressure signals. *Chem. Eng. Sci.* **1997**, *52*, 4447.

(32) Takens, F. *Lect. Notes Math.* **1981**, *898*, 366.

(33) Drahos, J.; Zahradnik, J.; Puncochar, M.; Fialova, M.; Bradka, F. Effect of operating conditions on the characteristics of pressure fluctuations in a bubble column. *Chem. Eng. Process.* **1991**, *29*, 107.

(34) Briens, L. A.; Briens, C. L. Cycle detection and characterization in chemical engineering. *AIChE J.* **2002**, *48* (5), 970.

(35) Khopkar, A. R.; Panaskar, S. S.; Pandit, A. B.; Ranade, V. V. Characterization of gas-liquid flows in stirred vessels using pressure and torque fluctuations. *Ind. Chem. Eng. Res.* **2005**, *44*, 3298–3311.

(36) Suntahnkar, A. A.; Ranade, V. V. *Dynamics of gas-liquid flow*; NCL Internal Report, **1997**.

(37) Press, W. H.; Teukolsy, S. A.; Vellering, W. T.; Flannery, B. P. *Numerical recepies in FOTRAN*; Cambridge University Press: New York, 1987.

(38) Hurst, H. E. Methods of using long-term storage in reservoirs. *Am. Soc. Chem. Eng.* **1951**, *116*, 770.

(39) Peters, E. E. *Fractral market analysis: Applying chaos theory to investment economics*; Wiley: New York, 1994.

(40) Kasat, G. R.; Khopkar, A. R.; Pandit, A. B.; Ranade, V. V. CFD simulations of liquid-phase mixing in solid−liquid stirred reactor. *Chem. Eng. Sci.* **2008**, *63*, 3877–3885.